Dimeric Electron Transport Materials and Their Use in Electrophotography

Zbig Tokarski[1], Ron Moudry[1], Kam Law[1], Nusrallah Jubran[1], Vytautas Getautis[2], Vygintas Jankauskas[2], Valentas Gaidelis[3], Edmundas Montrimas[3], and Jonas Sidaravicius[4]
[1]Samsung Information Systems America, Woodbury, Minnesota
[2]Kaunus University of Technology, Faculty of Chemical Technology, Kaunus, Lithuania
[3]Vilnius University, Department of Solid State Electronics, Vilnius, Lithuania
[4]Vilnius Gediminas Technical University, Vilnius, Lithuania

Abstract

Dimeric electron transport materials having the following general structure were developed.

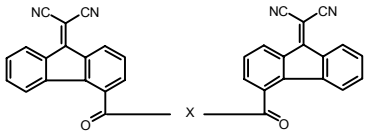

General Structure

All these derivatives were made in a three step reaction. First, 9-fluorenone-4-carboxylic acid was chlorinated with thionyl chloride to form 9-fluorenone-4-carbonyl chloride. Second, 9-fluorenone-4-carbonyl chloride was reacted with a diol or dithiol compounds to form a dimeric fluorenone intermediate. Finally, the intermediate was reacted with malononitrile to form the electron transport product. Fourteen new derivatives were made with different linkage groups, X. The final products were purified and their structures confirmed by proton NMR. The glass transition temperature (T_g) and electron mobility (μ) was measured for all viable derivatives. Single layer organic photoconductor constructions demonstrated the potential of these electron transport materials for electrophotography.

Introduction

The electrophotographic printer/copier market has an abundance of negatively charging, dual layer organic photoconductors (OPC) used to form latent images for negatively charged dry toner applications. Positively charging OPCs, on the other hand, are far less prevalent due to either the propensity of dry toners to be negatively charged, the difficulty in dip coating inverted dual layer OPCs, or the dearth of suitable electron transporting materials for single layer OPCs. These single layer organic photoconductors (OPC) utilize all of the components found in dual layer OPCs plus an extra material that facilitates the transport of electrons from the bulk to the positively charged OPC surface. These electroactive components function to generate electron-hole (*e*/h) charge pairs and facilitate transport of these charges to their perspective ground planes. A polymeric binder is required for mechanical durability and chemical phase compatibility. Electron mobility in single layer OPCs is 1-3 orders of magnitude slower than hole mobility and the possibility exists that both *e*/h mobility would diminish if the electron and hole transporting materials formed strong charge transfer complexes[1]. This paper presents the results of one attempt to develop electron transporting materials that have suitable mobilities and form weak charge transfer complexes.

There are serious problems encountered in preparation of single layer OPC caused by the crystallization of transporting materials and their solubility in liquid toners. The results of this paper present solutions to these problems.

Experimental

ETM Syntheses

The synthesis of these dimeric electron transport materials was done in three steps. First, 9-fluorenone-4-carboxylic acid is chlorinated with thionyl chloride to form 9-fluorenone-4-carbonyl chloride which is isolated and characterized. In the second step, 9-fluorenone-4-carbonyl chloride is reacted with diol or dithiol compounds at mole ratio 2:1 (fluorenone : diol) and the product is isolated and characterized. Finally, this intermediate is reacted with malononitrile to form the final product which was purified by recrystallizing several times.

The following fourteen compounds were prepared:

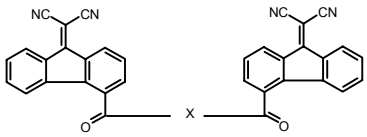

General Structure

where X equals the following bridging groups joining the electron active chromophore ends.

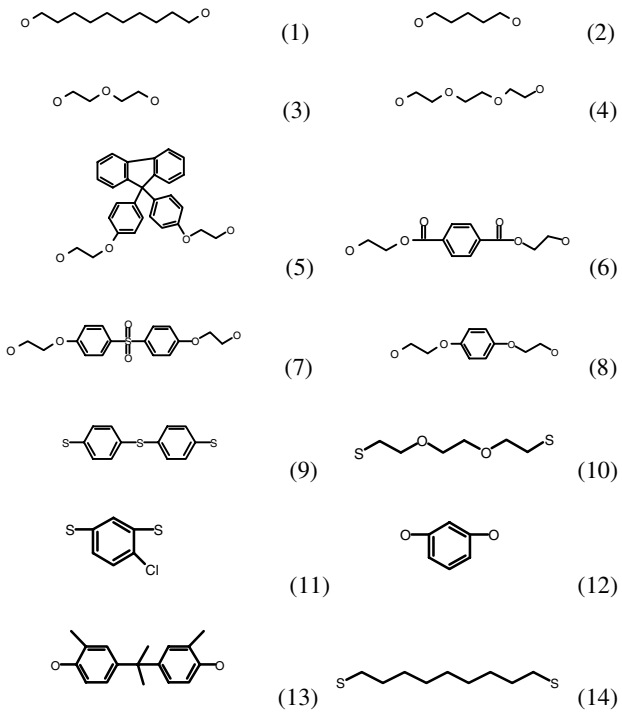

Electron Mobility Measurements

Charge carrier mobility measurements were performed on 5-10 μm thin films coated on an aluminized polyester substrate. The ETM to polycarbonate Z-type binder composition ratio was 1:1 (w/w).

The electron drift mobility was measured, by a xerographic time of flight technique (XTOF)[2], for only compounds 1 and 14 because the limited solubility of the other compounds prevented the measurement of their mobilities. Negative corona charging creates an electric field inside the ETM layer and charge carriers were generated at the layer surface by illuminating the sample with pulses from a nitrogen laser (pulse duration was 2 ns, wavelength 337 nm). The layer surface potential decreased 1-5 % of initial potential as a result of the pulse illumination. A capacitance probe, connected to the wide frequency band electrometer, measured the surface potential reduction rate, dU/dt. The transit time t_t was determined by the kink in the curve of the dU/dt transient in linear or double logarithmic scale. The drift mobility was calculated by the formula $\mu=d^2/U_0 \cdot t_t$, where d is the layer thickness and U_0 is the surface potential at the moment of illumination.

Electrostatic Cycling Measurements

Extended electrostatic cycling was performed on a test bed that is capable of evaluating 30 mm diameter, ring coated drums. This evaluation simulates accelerated electrostatic fatigue during extended printing by increasing the charge-discharge cycling frequency and decreasing the recovery time as compared to larger diameter drum formats. The drum rotates at a rate of 12.7 cm / sec (5 ips) and the location of each station in the tester is given in Table 1:

Table 1. Electrostatic Test Station Locations

Station	Degrees	Total Distance, cm	Total Time, sec
Erase Bar Center	0º	Initial, 0 cm	Initial, 0 s
Scorotron Charger	87.3º	2.28	0.18
Laser Strike	147.7º	3.86	0.304
Probe #1	173.2º	4.53	0.357
Probe #2	245.9º	6.43	0.506
Erase Bar Center	360º	9.42	0.742

All measurements were performed at ambient temperature and relative humidity. Electrostatic measurements were obtained as a compilation of diagnostic and long cycling tests.

1. Diagnostic Test: A charge acceptance, Vacc, and discharge voltage, Vdis, baseline was established by subjecting the samples to corona charging for three complete drum revolutions (laser off); discharging with the laser (780nm, 600dpi, 100% duty cycle) on the forth cycle; completely charged for the next three cycles; discharged with only the erase lamp @ 720nm on the eighth cycle to obtain the residual voltage, Vres; and, finally, completely charged for the last three cycles. The difference between the Vacc and Vdis on the third cycle is reported as the functional dark decay voltage, Vdd.
2. EXTENDED CYCLING: The drum was electrostatically cycled for 500 drum revolutions according to the following sequence per drum revolution. The drum was charged by the corona, the laser was cycled on and off (80-100º sections) to discharge a portion of the drum and, finally, the erase lamp discharged the whole drum in preparation for the next cycle. The first and third sections of the drum were never exposed to the laser while the second and fourth sections were always exposed. This pattern was repeated for a total of 500 drum revolutions and the data recorded for every 25th cycle.
3. The diagnostic test is re-run after the long cycling test.

Results and Discussion

Similar single-unit electron transport materials are described in the literature,[3] e.g., Xerox developed and investigated (4-n-butoxycarbony-9-fluorenylidene) malononitrile[4] as an electron transport material (structure below)

We report the basic physical properties of all these materials, the electron mobilities, and their usage as effective electron transport materials for electrophotography.

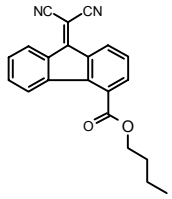

(4-n-butoxycarbonyl-9-fluorenylidene) malononitrile

Table 2. ETM melting point and T_g

Compound	m.p., ^{0}C	T_g, ^{0}C
1	133	38.0
2	163	70.8
3	155	58.0
4	157	55.0
5*	88	101.0
6**	90-200	62.0
7	110	87.0
8	166	53.0
9	114	90.0

* Overlapping T_m and T_g temperatures

** Polycrystalline

Table 2 lists the onset melting temperature and the glass transition temperature after solidification from the molten state.

Figure 1 contrasts the electron mobile nature of compound 14 in PCZ (1:1 w/w) to that of hole mobility in the same thin film. The drift in the charge acceptance voltage is observed in the time interval prior to 0 sec. A negatively charged film (lower curve) quickly decreased in surface potential after a short flash of UV light at time 0 sec whereas the potential of the positively charge film slowly decreased linearly with time. This demonstrates that electrons are mobile and holes are not mobile in this film. Electron movement from the thin generation region to the layer surface may cause the small potential jump at the illumination moment of the positively charged layer.

Figures 2 and 3 illustrate examples of the discharge transients as a function of initial applied voltage and the corresponding transit time derived, mobility field dependencies, respectively. The electron transport for compound 14 in PCZ, as seen in the figure, is dispersive in nature. In all the cases investigated, the mobility μ is approximated by the formula

$$\mu = \mu_0 e^{\alpha\sqrt{E}} \quad (1)$$

Here μ_0 is the extrapolated value for the zero field mobility α is Pool-Frenkel parameter and E is electric field strength. Table 3 lists the mobility defining parameters μ_0 and α values as well as the mobility values at the $6.4 \cdot 10^5$ V/cm field strength for ETM: PCZ (1:1 mass ratio) thin film constructions.

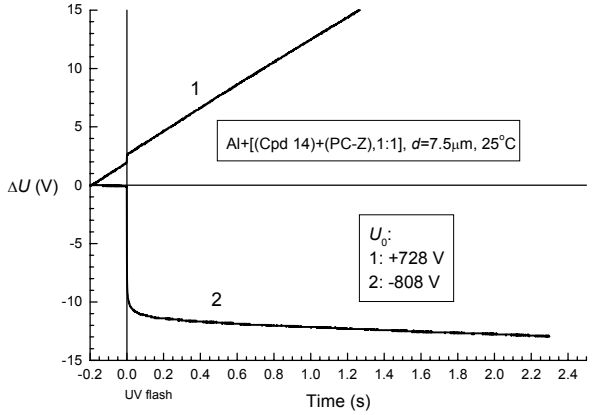

Figure 1. XTOF transient in integral mode for Cpd(14): PCZ (1:1)

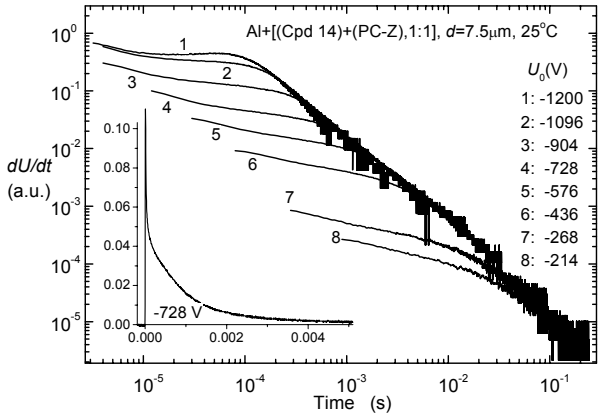

Figure 2. XTOF transient for compound (14): PCZ (1:1)

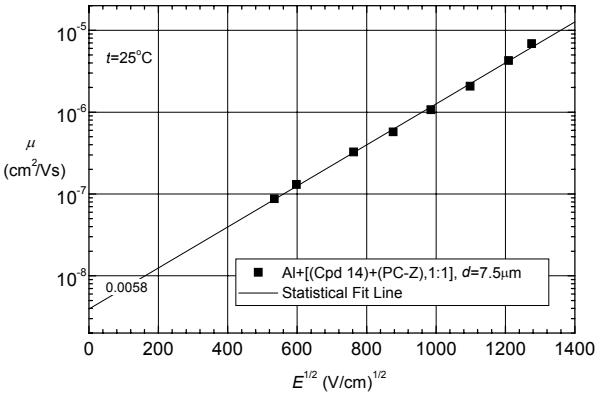

Figure 3. Electron mobility of compound (14) vs. field strength

Table 3. Electron Mobility via XTOF technique

Cpd	μ_0 (cm^2/V.s)	μ (cm^2/V.s) at 6.4x10^{5}V/cm	a (cm/V)$^{0.5}$
1	1.0 x 10^{-8}	1.4 x 10^{-7}	0.0047
14	0.38 x 10^{-8}	3.8 x 10^{-7}	0.0058
A	1.7 x 10^{-8}	20 x 10^{-7}	0.0062

A = (4-n-butoxycarbonyl-9-fluorenylidene) malononitrile

It is clear from the results in Table 3, that the mobility of the single-unit type of electron transporting material is ca. one order of magnitude higher than the dimeric-unit ETMs at an electrical field of 6.4 x 10^{-5} V/cm. One explanation for the lower mobilites is that the mass of the X bridging groups dilutes the amount of electron active chromophore added to the PCZ. However, the mass difference between the ETMs is too small to account for the entire difference in mobilities. Another explanation is that the molecular distribution of the active chromophores in the layer composition is not as favorable for electron transport as in the less sterically hindered, single-unit (4-n-butoxycarbonyl-9-fluorenylidene) malononitrile ETM.

Positive charging, single layer photoconductor constructions were ring coated onto 30 mm diameter anodized aluminum drum cores. The coating solution composition consisted of CGM : HTM : ETM : polyvinylbutyral binder at a ratio equal to 4.3 : 52.0 : 15.0 : 28.7 in chlorinated solvent. The electroactive components included oxytitanyl phthalocyanine CGM, MPCT-10 hole transport material from Mitsubishi Paper Mills, and ETM compounds 1, 4, 5, or 7. The dry OPC thickness was 10 µm.

Figures 4 and 5 illustrate the data output from the extended cycling (500 cycles) and diagnostic portions of the electrostatic cycling measurement, respectively. In Figure 5, the diagnostic test shows the results after electrostatically exercising the sample for 500 cycles.

Table 4 presents the electrostatic diagnostic test results for fresh drums and drums after 500 cycles. The values for the charge acceptance voltage (V_{acc}, probe #2 average voltage obtained from the third cycle), discharge voltage (V_{dis}, probe #2 average voltage obtained from the fourth cycle), functional dark decay voltage (V_{dd}, average voltage difference between probes 1 & 2 obtained from the third cycle), and the residual voltage (V_{res}, probe 2, average voltage obtained from the eighth cycle) are reported for fresh and electrostatically exercised samples.

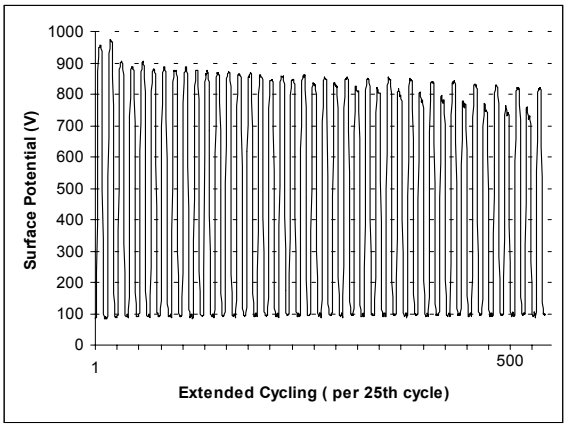

Figure 4. Extended cycling chart for single layer OPC using compound (1) as ETM

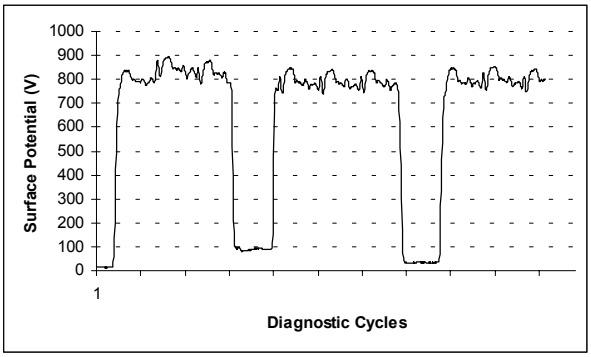

Figure 5. Cyclic chart at 500 cycles for single layer OPC using compound (1) as ETM

Table 4. Electrostatic cycling of single layer OPC

	Initial				After 500 cycles			
Cpd	V_{acc}	V_{dd}	V_{dis}	V_{res}	V_{acc}	V_{dd}	V_{dis}	V_{res}
1	999	22	91	27	799	26	90	33
4	518	57	28	19	446	62	32	12
5	932	20	95	42	780	11	99	44
7	1035	45	91	36	784	57	85	40
A*	905	29	61	21	618	60	58	22

The comparison compound, A*, in the previous table was (4-n-butoxycarbonyl-9-fluorenylidene) malononitrile. All of the new ETM samples showed a good initial charge acceptance voltage that changed by only 10-20% of the initial value after extended cycling. The discharge and residual voltages remained low and did not change with cycling. Electron trapping may cause a small decrease in the charge acceptance voltage at the beginning of cycling. This again may be the result of an unfavorable molecular distribution in the layer composition. Despite this shortcoming these materials are better suited for single layer OPC preparation as compared to the single-unit analogs because of stability to crystallization and the effects of liquid developer.

Conclusion

A series of dimeric electron transport compounds have been prepared in a 3 step reaction. First 9-fluorenone-4-carboxylic acid was chlorinated with thionyl chloride to form 9-fluorenone-4-carbonyl chloride which was reacted with linkage groups to form dimeric intermediate. This intermediate was then reacted with malononitrile to form the final product which was recrystallized and its structure was confirmed by proton NMR. The xerographic time of flight measurements of these ETMs showed electron mobilities of ca. 10^{-7} cm^2/Vs, only a 10 fold lower mobility than the extractable single-unit ETM material. A single layer OPC drum using these electron transport materials showed good electrostatic performance (high charge

acceptance, low discharge and low dark decay) which indicates the usefulness of these dimeric ETMs in liquid electrophotography.

References

1. F. Sugai, Y. Inagaki, US Patent 6,346,355
2. E. Montrimas, V. Gaidelis, A. Pazera, "The discharge kinetics of negatively charged Se electrophotographic layers," Lithuanian Journal of Physics, 6, p. 569-576 (1966).
3. Organic Photoreceptors for Electrophotography, edited by Paul M. Boresenberger and David s. Weiss.
4. US patent 4,559,287

Biography

Nusrallah Jubran received his B.S degree in Chemistry from the Hebrew University at Jerusalem, Israel in 1977, a M.S in Chemistry from the Weismann Institute at Rehovot, Israel in 1979, and a Ph.D. in Chemistry from Ben-Gurion University at Beer-Sheva, Israel in 1985. Since 2000 he has worked as a staff chemist in Samsung Digital Printing Solution Lab in Woodbury, MN. His current research activities focus on the development and scale up of novel OPC materials for electrophotography. Prior to joining Samsung, he worked for a period of 13 years with 3M/Imation on several imaging technologies. He is a member of the IS&T.

Correspondence on this paper should be e-mailed to njubran@mn.sisa.samsung.com